Learning Optical Maps in Liquid Xenon Detector with Poisson Likelihood Loss

Shixiao Liang
Department of Physics and Astronomy
Rice University
liangsx@rice.edu

Christopher Tunnell
Department of Physics and Astronomy
Rice University
tunnell@rice.edu

Abstract

Dual-phase liquid xenon time projection chambers (LXeTPC) have been successfully applied in rare event searches in astroparticle physics because of their ability to reach low backgrounds and detect small scintillation signals with photosensors. Accurate modeling of optical properties is essential for reconstructing particle interactions within these detectors as well as for developing data selection criteria. This is commonly achieved with discretized maps derived from Monte Carlo simulation or approximated with empirical analytical models. In this work, we employ a novel approach to this using a neural network trained with a Poisson log-likelihood ratio loss to model the mapping from light source location to the expected light intensity for each photosensor. We demonstrate its effectiveness by integrating it into a likelihood fitter for position reconstruction, simultaneously providing insights into the uncertainty associated with the reconstructed position.

1 Introduction

Dual-phase liquid xenon time projection chamber (LXeTPC) detectors are used to search for rare events in astroparticle physics such as dark matter [1, 5, 8, 12] and neutrinoless double-beta decay [3, 4, 7] searches because of their ability to reach low background levels, discriminate between signals and backgrounds, and provide 3D position reconstruction of a single particle interaction within the detector. When an interaction occurs inside the liquid xenon target in the detector, a prompt scintillation (S1) signal is observed by two arrays of photosensors at the top and bottom of the detector, and a secondary scintillation (S2) signal is generated when electrons released from the interaction site are drifted to the top of the detector by an applied electric field. Since the S2 signals are generated near the top photosensor array, the light distribution is sensitive to the light source location. Consequently, this sensitivity allows for accurate reconstruction of the positions of the S2 signals and data selection based on the light distribution pattern.

Modeling the optical properties of the detector is crucial for the development of S2 position reconstruction methods. This involves estimating the expected light intensity for each photosensor in response to the S2 signal's position. This is a challenging task for LXeTPC detectors, primarily because these optical properties can vary among detectors and direct measurements become impractical once the detector is commissioned. One common approach is to generate discretized maps through Monte Carlo optical simulations, which can effectively capture small-scale structures when pixel sizes are sufficiently small. These maps can serve as inputs for expediting photosensor waveform simulations [10], reducing the need for computationally intensive optical simulations. However, this method relies heavily on simulations and can pose challenges when constructing likelihood fitters. Therefore, position reconstruction methods based on this modeling approach often involve training machine learning models on simulated S2 signals to learn the mapping from light distribution patterns to S2 positions [6, 11]. Alternatively, empirical analytical models offer a smoother, easily differentiable function for likelihood fitting in position reconstruction [2, 14, 15]. These models can

Machine Learning and the Physical Sciences Workshop, NeurIPS 2023.

be parameterized using either simulated or experimental data, but they may oversimplify detector intricacies, such as fine structures caused by electrode-induced light obstructions.

In this study, we explore a new option for modeling the optical map that can provide an advantage over both discretized maps and empirical analytical models. A neural network model should be able to learn fine details in the optical map and can give the gradient necessary for a likelihood fitter if the activation function is appropriately selected. We trained a multilayer perceptron (MLP) model on simulated S2 patterns with a likelihood-based loss function and implemented a likelihood fitter for position reconstruction using the trained MLP model[1]. We show that the assessment of reconstructed position uncertainty can be achieved by conducting a likelihood scan with the MLP model.

2 Method

2.1 Learning the optical map

Learning the optical map with neural network models requires understanding the S2 generation process to construct an appropriate loss function. This challenge is also encountered when fitting empirical models, as previously investigated in Refs. [2, 14, 15]. For photosensor i with an expected light intensity of λ_i, the observed signal k_i can be sampled as follows:

$$k_i \sim F(\mu_i, \theta), \text{ where } \mu_i \sim \text{Poisson}(\lambda_i)\,. \tag{1}$$

Here, $F(\mu_i, \theta)$ represents a distribution that accounts for the limited resolution of photosensors, commonly approximated using a normal distribution, while the Poisson distribution models the photon counting process. Both k_i and λ_i have units of photoelectrons (PE). λ_i can be expressed as the product of $H_i(x, y)$—a function of the 2D coordinate on a plane parallel to the top photosensor array that represents the fraction of light observed by photosensor i—and the expectation value of the total amount of signal observed by the photosensor array, $k_T = \sum_i k_i$. This latter quantity is dependent of the energy of the interaction within the detector:

$$\lambda_i = k_T H_i(x,\, y)\,. \tag{2}$$

Our goal is to train a neural network model to learn $H_i(x, y)$. To achieve this, an ideal loss function should accurately capture both the Poisson process and the broadening effect. After experimentation, we discovered that employing a loss function based on a log-likelihood ratio effectively serves this purpose:

$$\mathcal{L} = -2 \sum_i [\log \mathcal{P}(k_i;\, \lambda_i) - \log \mathcal{P}(\lambda_i;\, \lambda_i)]\,, \tag{3}$$

where $\log \mathcal{P}(k_i;\, \lambda_i)$ is the Poisson log-likelihood:

$$\log \mathcal{P}(k_i;\, \lambda_i) = k_i \log(\lambda_i) - \log \Gamma(k_i + 1) - \lambda_i\,. \tag{4}$$

Note that the domain of the factorial operation has been extended to the positive real numbers by use of the gamma function.

We used an MLP model with a 2-dimensional input, representing the x and y coordinates of the S2 signal, and a 253-dimensional output, corresponding to the number of photosensors in the upper photosensor array of the considered LXeTPC detector. The MLP model has 3 hidden layers of dimensions 20, 60, and 180. The MLP architecture includes three hidden layers with dimensions of 20, 60, and 180, respectively. To introduce non-linearity while ensuring differentiability, we applied the Exponential Linear Unit (ELU) activation function between the hidden layers, and the output layer used a sigmoid activation function to constrain the outputs to lie between 0 and 1. The MLP model was implemented and trained using Pytorch [13].

[1] https://github.com/DidactsOrg/nns2maps

The data used for training and evaluating MLP model we generated synthetic S2 data using a simulation method detailed in [11], which uses an empirical model for $H_i(x, y)$ and assumes $F(\mu_i, \theta)$ as a normal distribution. The S2 positions were uniformly distributed over the detector area and the k_T of the S2s were around 4500 PE. As illustrated in Figure 1, the Poisson fluctuation and broadening effect become more pronounced when λ_i is small.

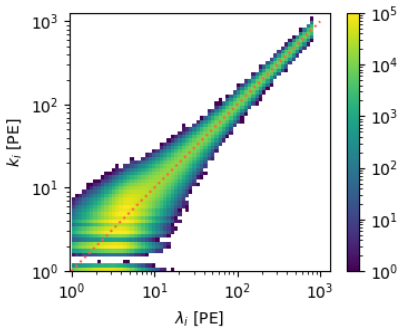

Figure 1: A comparison of expectation value of the signal λ_i and simulated observed value k_i in the synthetic data set.

2.2 Likelihood fitter with trained model

In previous studies, likelihood fitters for position reconstruction relied on empirical analytical models, enabling the gradient on the loss function to propagate smoothly to the input [2, 14, 15]. A trained MLP model also allows the gradient to flow from the loss function to the input—specifically the x and y coordinates of a test position. By running an optimizer, in our case the built-in stochastic gradient descent optimizer in Pytorch, on the input data, we can find a test position that has the lowest likelihood loss within the deep learning framework.

The likelihood fitter minimizes the log-likelihood ratio in Eq. 3. The starting point was set at the center position of the photosensor with the highest intensity. The iteration was terminated when the test position moved less than 1 mm in distance for three consecutive iterations.

3 Results

The goal of training the MLP model is to learn $H_i(x, y)$ for the prediction of λ_i. Since the training data is derived from simulations, it provides us with the true values of λ_i for comparison. Another MLP model of the same architecture was trained using the Mean Squared Error (MSE) loss, a commonly used loss function for regression problems, and its performance was compared with the model trained using the log-likelihood ratio.

As shown in Figure 2, both models are capable of predicting λ_i, but the one trained on the likelihood ratio outperforms the MSE-trained model. The model trained on MSE loss performs less effectively for smaller values of λ_i because the loss function struggles to capture Poisson fluctuations. However, for larger λ_i, both models perform reasonably well. This observation aligns with expectations, as the log-likelihood ratio effectively approximates a χ^2 loss, which behaves similarly to the MSE loss when the Poisson distribution is approximated by a normal distribution.

Figure 3 illustrates the outcome of applying the likelihood fitter to a simulated S2 signal. The reconstructed position matches the simulated position well. The result of the likelihood scan for this particular S2 signal reveals that the log-likelihood ratio returns small values for positions near the true position, indicating that the predicted λ_i in this region matches the observed values better than the region further away from the true position. Note that the values outside the detector's boundaries are not meaningful as S2 signals cannot physically occur outside the detector.

4 Conclusion and Discussion

We trained and tested an MLP model using simulated S2 data, showcasing its ability to learn optical mappings for position reconstruction. This method is not limited to simulations; it can be extended to real data for practical applications and provide inputs for waveform simulators.

In conclusion, our study demonstrates the promise of MLP models in optical mapping and likelihood fitting, paving the way for advancements in particle detector position reconstruction.

Limitations

This work relies on simulations that employ simplified models for optical maps and photosensor responses.

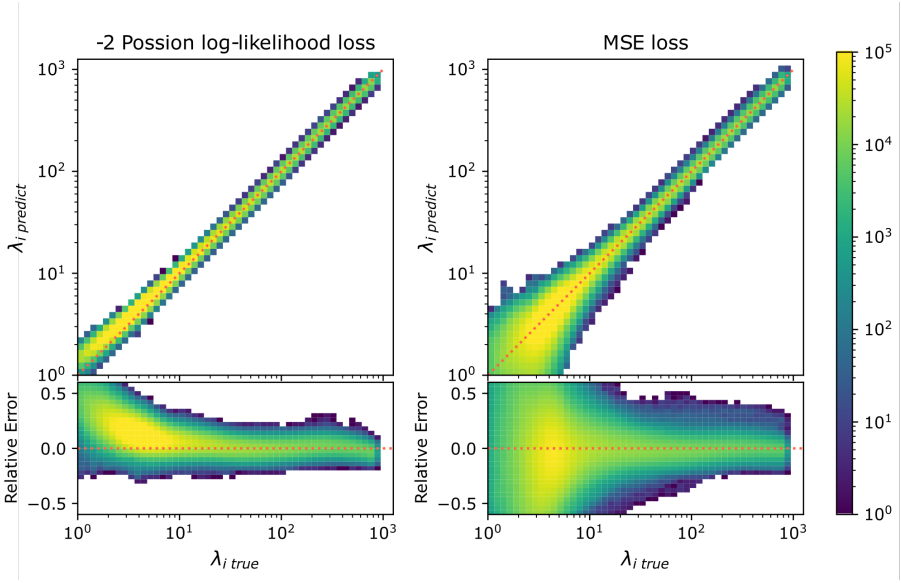

Figure 2: Predicted λ_i and the relative error vs true λ_i for an MLP model trained on log-likelihood ratio loss (left) and Mean Squared Error (MSE) loss (right).

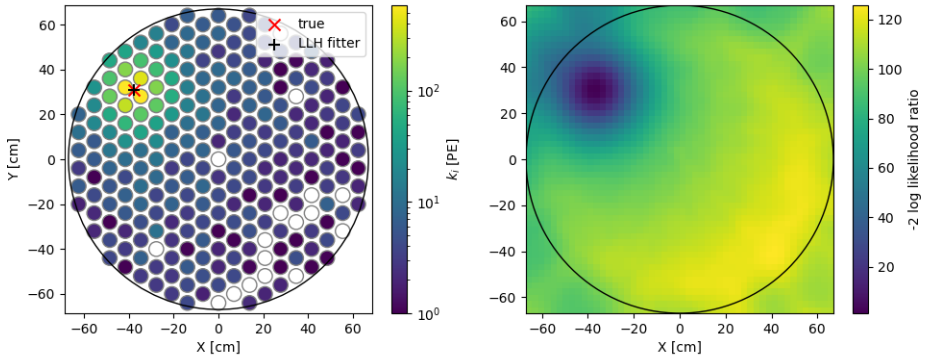

Figure 3: (Left) An example of reconstructed position using a likelihood fitter built with the trained MLP model. The smaller circles represent the photosensors and the color marks k_i for each photosensor. (Right) The result of a likelihood scan using the trained MLP model. The black circle marks the boundary of the considered LXeTPC detector.

Future works

Future research should focus on improving the modeling of photosensor broadening effects, which vary among individual photosensors and could have complex dependencies on μ_i . Additionally, there is the potential to merge our two neural network models——mapping S2 light distribution to position and vice versa—either as an autoencoder or using normalizing flow models such as invertible neural networks [9].

Boarder impact

This methodology extends to real-world detector applications and the loss function can be applied to tasks involving Poisson-based signal generation. This work does not pose any negative societal impacts.

5 Acknowledgement

This work is supported by the National Science Foundation through award 1940209. The authors would like to thank Juehang Qin, Dorian Amaral and Aobo Li for insightful discussions and feedback. ChatGPT was used to enhance the writing of this paper.

References

[1] J. Aalbers et al. First Dark Matter Search Results from the LUX-ZEPLIN (LZ) Experiment. *Phys. Rev. Lett.*, 131(4):041002, 2023. doi: 10.1103/PhysRevLett.131.041002.

[2] D. S. Akerib et al. Position Reconstruction in LUX. *JINST*, 13(02):P02001, 2018. doi: 10.1088/1748-0221/13/02/P02001.

[3] D. S. Akerib et al. Projected sensitivity of the LUX-ZEPLIN experiment to the $0\nu\beta\beta$ decay of ^{136}Xe. *Phys. Rev. C*, 102(1):014602, 2020. doi: 10.1103/PhysRevC.102.014602.

[4] D. S. Akerib et al. Projected sensitivity of the LUX-ZEPLIN experiment to the two-neutrino and neutrinoless double β decays of ^{134}Xe. *Phys. Rev. C*, 104(6):065501, 2021. doi: 10.1103/PhysRevC.104.065501.

[5] E. Aprile et al. Dark Matter Search Results from a One Ton-Year Exposure of XENON1T. *Phys. Rev. Lett.*, 121(11):111302, 2018. doi: 10.1103/PhysRevLett.121.111302.

[6] E. Aprile et al. XENON1T Dark Matter Data Analysis: Signal Reconstruction, Calibration and Event Selection. *Phys. Rev. D*, 100(5):052014, 2019. doi: 10.1103/PhysRevD.100.052014.

[7] E. Aprile et al. Double-Weak Decays of ^{124}Xe and ^{136}Xe in the XENON1T and XENONnT Experiments. *Phys. Rev. C*, 106(2):024328, 2022. doi: 10.1103/PhysRevC.106.024328.

[8] E. Aprile et al. First Dark Matter Search with Nuclear Recoils from the XENONnT Experiment. *Phys. Rev. Lett.*, 131(4):041003, 2023. doi: 10.1103/PhysRevLett.131.041003.

[9] L. Ardizzone, J. Kruse, S. Wirkert, D. Rahner, E. W. Pellegrini, R. S. Klessen, L. Maier-Hein, C. Rother, and U. Köthe. Analyzing inverse problems with invertible neural networks. *arXiv preprint arXiv:1808.04730*, 2018.

[10] P. Gaemers et al. Xenonnt/wfsim: v1.0.2, Oct. 2022. URL `https://doi.org/10.5281/zenodo.7216324`.

[11] S. Liang, , et al. Domain-Informed Neural Networks for Interaction Localization Within Astroparticle Experiments. *Front. Artif. Intell.*, 5:832909, 2022. doi: 10.3389/frai.2022.832909.

[12] Y. Meng et al. Dark Matter Search Results from the PandaX-4T Commissioning Run. *Phys. Rev. Lett.*, 127(26):261802, 2021. doi: 10.1103/PhysRevLett.127.261802.

[13] A. Paszke, S. Gross, F. Massa, A. Lerer, J. Bradbury, G. Chanan, T. Killeen, Z. Lin, N. Gimelshein, L. Antiga, et al. Pytorch: An imperative style, high-performance deep learning library. *Advances in neural information processing systems*, 32, 2019.

[14] V. N. Solovov et al. Position Reconstruction in a Dual Phase Xenon Scintillation Detector. *IEEE Trans. Nucl. Sci.*, 59:3286–3293, 2012. doi: 10.1109/TNS.2012.2221742.

[15] D. Zhang et al. Horizontal position reconstruction in PandaX-II. *JINST*, 16(11):P11040, 2021. doi: 10.1088/1748-0221/16/11/P11040.